A Two-Stage Resilience Enhancement for Distribution Systems Under Hurricane Attacks

Yichen Shen, *Student Member, IEEE*, Chenghong Gu, *Member, IEEE*, Zhibo Ma, Xinhe Yang, *Student Member, IEEE*, and Pengfei Zhao, *Student Member, IEEE*

***Abstract*—Hurricane events can cause severe consequences to the secure supply of electricity systems. This article designs a novel two-stage approach to minimize hurricane impact on distribution networks by automatic system operation. A dynamic hurricane model is developed, which has a variational wind intensity and moving path. The article then presents a two-stage resilience enhancement scheme that considers predisaster strengthening and postcatastrophe system reconfiguration. The pre-disaster stage evaluates load importance by an improved PageRank algorithm to help deploy the strengthening scheme precisely. Then, a combined soft open point and networked microgrid strategy is applied to enhance system resilience. Load curtailment is quantified considering both power unbalancing and the impact of line overloading. To promote computational efficiency, particle swarm optimization is applied to solve the designed model. A 33-bus electricity system is employed to demonstrate the effectiveness of the proposed method. The results clearly illustrate that the impact of hurricanes on load curtailment, which can be significantly reduced by appropriate network reconfiguration strategies. This model provides system operators a powerful tool to enhance the resilience of distribution systems against extreme hurricane events, reducing load curtailment.**

***Index Terms*—Electric system, hurricane events, load loss, reconfiguration.**

NOMENCLATURE

$P_{f,\text{Pylon},i}$	Failure probability of the pylons.
$P_{f,\text{Poles},j}$	Failure probability of the poles.
$P_{f,\text{Conductors},j}$	Failure probability of the conductors.
F_{wind}, F_{force}	Wind loading on the conductor and the limit of force on transmission lines.
$P_{f,\text{Debris}}$	Probability of tree wind-throw near to the *j*th conductor.
S_j	Wind intensity at conductor *j*.
D_H	Tree diameter at its breast height.
k_s	Terrain effect factor that determined by local land cover information.
a_s, b_s, c_s	Constants for tree species.
$P_{f,\text{br}}$	Failure probability for overall system branches.
$c(\omega_i, \omega_j)$	Distance between scenario i and j.
$LL_{\text{line}}, LL_{\text{Buck}}, LL_{\text{iso}}$	Load curtailment owing to overloading line, tower buckling, and isolated load.
D, F	Sets of damaged and functional branches at the kth failure scenario.
$P\text{best}_i$	Best position experienced by ith particle.
$G\text{best}_i$	Best particle of the entire population.
V_i^t	Velocity of ith particle at time t.
x_i^t	Position of ith particle at time t.
α	Inertia weights of the stochastic acceleration terms.
β_1, β_2	Weighting factors of the stochastic acceleration terms.
r_1, r_2	Numbers randomly from a uniform distribution [0,1].
I_c, V_c	Current and voltage constraint of system branches.
$S(V_i)$	Sigmoid limiting transformation.
$w_{(v,u)}^{\text{in}}, w_{(v,u)}^{\text{out}}$	Importance of the number of inlinks and outlinks.
I_u, I_p	Number of inlinks of page u and page p.
O_u, O_p	Number of outlinks of page u and page p.
$e_x^{\text{in}}, e_x^{\text{out}}$	Injected energy and outlet energy.
$\text{PR}(u)$	Weight of system nodes.
f_{dev}	Voltage deviation owing to SOP.
$U_{t,i}$	Voltage of branches with SOP.

Manuscript received September 30, 2019; revised February 24, 2020 and April 28, 2020; accepted May 19, 2020. *(Corresponding author: Chenghong Gu.)*

Yichen Shen, Chenghong Gu, Xinhe Yang, and Pengfei Zhao are with the University of Bath, Bath BA2 7AY, U.K. (e-mail: ys884@bath.ac.uk; c.gu@bath.ac.uk; xin.yang2@bath.ac.uk; pz293@bath.ac.uk).

Zhibo Ma is with the National Grid, London WC2N 5EH, U.K. (e-mail: zhibo.ma@nationalgrideso.com).

Digital Object Identifier 10.1109/JSYST.2020.2997186

I. INTRODUCTION

DUE to the climate change, low-probability high-impact natural events could cause severe consequences to electricity systems. Because any failures of the distribution systems may cause significant energy loss, the security of the electricity system has to be assessed and managed properly. Due to that severe hurricane events can damage pylons and distribution lines, so the behaviours of the electricity system under hurricane attacks should be investigated with high priority. Thus, more concerns are paid to constructing resilient distribution systems. *Resilience* describes the capability of an object to fully recover to its original state after severe disruptions. Referred to power systems, resilience defines the ability for the system to restore its full functionality after disruptions, i.e., in networks or generation supply. Resilience enhancement strategy can be divided into two stages: the predisaster strengthen stage and the postdisaster recovery stage.

For the predisaster strengthening stage, system behaviors under severe hurricanes need to be investigated first. To quantify system response, a common method is to use operation cost or load shedding cost as key features in the literature [1], [2]. However, these metrics cannot directly reflect the decrease in system capability to satisfy load demand. Based on the analysis of system behaviors, a targeted hardening strategy is developed to improve distribution system reliability, which involves strengthening important distribution poles as well as poles with a high probability of failure by identifying risk-critical parts of the system [3]. A trilevel optimization model that considers the failure probability of hardened components was presented in [4]. According to hardening costs and weather parameters, there are three different hardening strategies for each line to strengthen enhancement.

For the postdisaster recovery stage, based on various types of switches, medium-voltage (MV) distribution systems can be easily reconfigured. MV distribution networks are usually operated in a radial configuration, which allows the use of switch operations to offer efficient and inexpensive protection schemes as well as providing fast fault isolation. Furthermore, microgrids (MGs) can be scheduled to restore system functionality as well. To construct resilient distribution systems, Schneider *et al.* [5] presented an emergency restoration method to provide an emergency power supply to critical loads facing extreme natural catastrophes. A self-recovery method that sectionalizes the distribution system into MG was presented in [6]. According to this method, the on-outage portion of the distribution system will be optimally sectionalized into self-supplied MGs, and then the outputs of dispatchable distributed generators (DGs) will be rescheduled accordingly. Consequently, a reliable power supply is provided to the maximum loads continuously. Optimally scheduling of available crews to minimize the cumulative duration of the customer interruptions can also reduce the impact of postdisasters [7]. To solve this problem, the repair and restoration process can be modeled as a scheduling problem with soft precedence constraints, and, subsequently, the problem is formulated as a scheduling problem. Cao *et al.* [8] provided a soft open point (SOP)-based reconfiguration scheme to minimize the power loss of the distribution system. To mitigate the propagation system fault, the fast fault recovery mode of SOP is introduced.

Generally, as an important type of extreme events, hurricanes can result in failures in distribution systems by causing fallen trees, fly debris, and direct damage to pylons. Hence, compared with transmission systems with less possible fly debris, distribution systems are more vulnerable to hurricane attacks [9]. However, regarding strengthening strategies, most work mainly considers the physical strengthening schemes of lines but ignore the necessary supply of system vulnerable load [2], [3]. A comprehensive method to combine prestrengthening and post-reconfiguration should be developed to efficiently manage systems for resilience enhancement.

This article investigates the resilience enhancement of the distribution system based on SOPs and networked MGs under hurricane events. A dynamic hurricane model with time-series intensity is deployed. Hurricane event is modeled as a moving circular region with time-varying wind profiles. A failure scenario generation and reduction algorithms are developed to simulate possible hurricane-inducing system faults. Different from previous papers that classify load curtailment by investigating unbalanced supply and demand, this proposed method investigates the loss of load demand by investigating unsatisfied demand and overloaded transmission lines.

The main contributions of this article are as follows.

1) Based on the coordination of SOPs and networked MGs, a two-stage resilience enhancement scheme is presented, which considers predisaster strengthening and postcatastrophe system reconfiguration.
2) The predisaster stage evaluates load importance by an improved PageRank algorithm to help deploy strengthening scheme precisely.
3) The damaged system cannot be reconfigured by this method, whereas the traditional reconfiguration can only mitigate the power loss.
4) The hurricane model is better dynamically modeled and has a variational wind intensity and a moving path.
5) The load curtailment due to hurricane attacks is more precisely described by considering both unbalanced load demand and the impact of line overloading.

The rest of this article is organized as follows. Section II investigates the hurricane response of the electricity system. In Section III, the reconfiguration scheme is studied. A case study is presented in Section IV. Finally, Section V concludes this article.

II. Impact Evaluation of Hurricane Stress

Because hurricane events mainly affect the distribution system's branches, this section is organized to investigate the hurricane behaviours on distribution poles, conductors, and pylons. Accordingly, a probabilistic model that describes system branch loss is proposed. Subsequently, the load curtailment caused by branch loss is then used as the main metric to quantify system behaviors.

A. Distribution Circuits' Fragility

For typical distribution systems, there are three types of components that are particularly vulnerable to severe hurricane events: supporting towers (or pylon), distribution poles, and distribution conductors.

The failure probability of the pylons can be classified as [10]

$$P_{f,\mathrm{Pylon},i} = \min\left\{2 \times 10^{-7} e^{0.0824 x_i}, 1\right\} \tag{1}$$

where x_i represents the wind speed of hurricane at the *i*th supporting pylon.

The failure probability of the *j*th distribution pole is given as [10]

$$P_{f,\mathrm{Poles},j} = \min\left\{0.0001 e^{0.0421 x_j}, 1\right\}. \tag{2}$$

Considering wind loading and tree wind-throw, the failure probability of conductors between transmission poles is [11]

$$P_{f,\mathrm{Conductors},k} = \max\left\{P_{f,\mathrm{wind},k}, P_{f,\mathrm{Debris},k}\right\} \tag{3}$$

$$P_{f,\mathrm{wind},k} = \min\left\{F_{\mathrm{wind},k}/F_{\mathrm{force},k}, 1\right\} \tag{4}$$

where F_{wind} refers to the wind loading on the conductor, and F_{force} is the limit of force on transmission lines. $P_{f,\mathrm{Debris}}$ is the probability of tree wind-throw near to the *j*th conductor.

The $P_{f,\mathrm{Debris}}$ can be classified as [2]

$$P_{f,\mathrm{Debris}} = \frac{e^{h(S_k)}}{1+e^{h(S_k)}} \tag{5}$$

$$h\left(S_k\right) = a_s + k_s\left(c_s S_k\right) D_H^{b_s} \tag{6}$$

where S_k is the wind intensity at conductor *k*, D_H is the tree diameter at its breast height, k_s is a terrain effect factor that is determined by local land cover information, and a_s, b_s, and c_s are constants for tree species.

Consequently, the failure probability for overall system branches $P_{f,\mathrm{br}}$ is

$$P_{f,\mathrm{br}_{ijk}} = 1 - \prod_{i=1}^{n}\left(1-P_{f,\mathrm{Pylon}}\right)\prod_{j=1}^{m}\left(1-P_{f,\mathrm{Poles}}\right) \times \prod_{k=1}^{l}\left(1-P_{f,\mathrm{Conductors}}\right). \tag{7}$$

B. Failure Scenarios

Each branch can be in either functional or damaged state in the next time period. Hence, the kth failure scenario is [4]

$$P_{f,Sk} = \prod_{i=1}^{D} P_{f,\mathrm{br}i}\prod_{j=1}^{F}\left(1-P_{f,\mathrm{br}j}\right) \tag{8}$$

where D and F are the sets of damaged and functional branches at the kth failure scenario, respectively. $P_{f,\mathrm{br}i}$ is the probability of the ith branch to be damaged in the next time stage.

However, to generate failure scenarios, there is an unduly amount of possibilities if considering all possible combinations of failure branches. For a system with N branches, there would be 2^N possible failure scenarios. Since this complex problem cannot be solved by normal approaches, proper scenario generation and reduction algorithms are needed. In this article, when possible failure scenarios are less than the manageable size σ_{man}, the scenario generation algorithm would be applied. When failure scenarios are larger than the selected threshold σ_{thr}, the scenario reduction mode is [5]

$$c\left(\omega_i, \omega_j\right) = \left|\omega_i - \omega_j\right| \tag{9}$$

$$\min\left\{\sum_{\mu\in j} p_\mu \min c\left(\omega_i, \omega_j\right),\ j' = S - s\right\} \tag{10}$$

$$\min_{l\in\{1,\ldots,S\}} p_l \min c\left(\omega_l, \omega_j\right). \tag{11}$$

The selected threshold and manageable size are 100 and 500, respectively. For (9)–(11), the relative closeness to other scenarios and scenario's own probabilities are considered as the main metrics to quantify reduction algorithm's efficiency. Subsequently, $c(\omega_i, \omega_j)$ represents the distance between scenario i and j, and *S* equals the initial set of scenarios for reduction algorithms. Since j denotes optimal delated scenarios, j' would be the fixed cardinality. The final version of scenario reduction algorithm is given in (11), which not only considers the probability p_l, but also considers the distance between scenarios $c(\omega_i, \omega_j)$. Accordingly, scenarios with similar or with lower probability would be filtered.

C. Load Curtailment

This scheme mainly considers load curtailment owing to hurricane attack in two aspects: First, the decrease in generators' capacity caused by pylon buckling or isolated loads. On the other hand, when line failure occurs (including all types of distribution circuit's damage), other lines would be overloaded due to increasing power flow, and proper load curtailment is required to ease the burden. This article curtails load demand based on demand sensitivity factor between branches and nodes.

The power flow equation can be expressed as

$$\dot{V}_i^{k+1} = \frac{\frac{P_i - jQ_i}{\widehat{\dot{V}_i^k}} - \sum_{j=1}^{i-1} Y_{ij}\dot{V}_j^{k+1} - \sum_{j=i+1}^{n} Y_{ij}\dot{V}_j^{k}}{Y_{ii}} \tag{12}$$

where *S* is the injected complex power, P_{gi} is the real power produced by the generator linking to bus i, Q_{gi} is the reactive power produced by the generator linking to bus i, P_{di} is the real power load of bus i, Q_{di} is the reactive power load of bus i, and *Y* is the impedance and admittance matrix.

The load curtailment would be assessed as

$$LL_{\mathrm{line}} = \sum_{k=1}^{n} LL_{\mathrm{line}} + \sum_{k=1}^{m} LL_{\mathrm{Buck}} + LL_{\mathrm{iso}} \tag{13}$$

where n is the number of overloading transmission line, m is the number of buckling turbine tower, and LL_{line}, LL_{Buck}, and LL_{iso} are the load curtailments owing to overloading line, tower buckling, and isolated load, respectively.

D. Hurricane Modeling

Based on [2], [12], and [13], this article proposes a dynamic hurricane model that maintains a variable wind profile (position and intensity). Referring to the response of energy systems, the typical hurricane modeling has two features: moving path and variational wind intensity [2]–[4]. Since the inner area of a hurricane can have different wind intensities, our model divides that area into three concentric circular regions, and, subsequently, each region maintains different wind intensities. Consequently, the affected lines of each *d* time can be distinguished [17].

In the aftermath of extreme hurricane events, aiming to recover system functionality as much as possible, the postcatastrophe system reconfiguration should be considered. In this section, an improved system reconfiguration scheme is proposed based on SOPs and networked MGs. Particle swarm optimization (PSO) is applied to enhance computational efficiency.

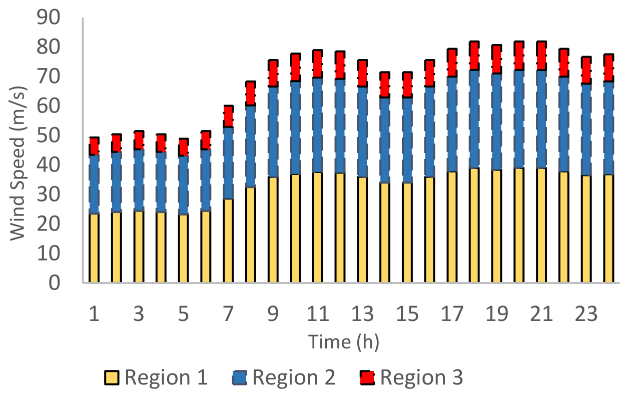

Fig. 1. Time-varying wind profiles.

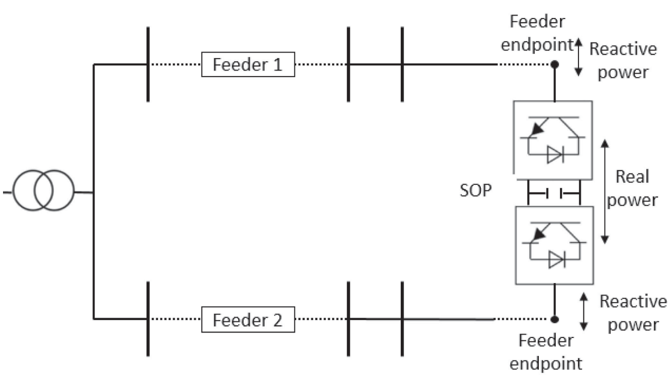

Fig. 2. The operational principle of SOPs.

The combination of system reconfiguration with support components, SOP and networked MGs, is introduced in details. The proposed reconfiguration strategy is divided into two stages: First, it deploys networked MGs to critical loads based on the PageRank algorithm. Then, it reconfigures the system to minimize curtailed load due to hurricane attack. If load isolation or islanded subsystem appears, network MGs will be scheduled to supply these islands when it is possible. Fig. 1 describes the wind speed variation in three regions of the hurricane; the wind speed is low during early morning and middle of the day but high during later morning and evening time.

E. SOPs and Networked MGs

Regarding extreme events, the post-disaster system cannot allow switch operation and further reconfiguration, since damaged branches cannot be switched ON again. Thus, in this article, SOPs are installed to provide the possibility of reconfiguration. And since SOPs are normally grounded, this article assumes that they would not be affected by hurricane stress and can only be switched ON at the postdisaster stage.

As Fig. 2 illustrates, on the basis of back-to-back voltage-source controllers (VSCs), SOP is deployed in place of normally open points to provide active power control, reactive power compensation, and voltage regulation under fault conditions of system operations [8], [14]. Referring to normal system operation condition, SOP can be operated in two modes: power flow control mode and supply restoration mode. The first mode can not only provide a dual closed-loop current-controlled strategy but also regulate the active and reactive powers, whereas the second restoration mode can benefit nearby loads with fast power supply recovery [8].

The voltage deviation offered by SOP would be

$$f_{\text{dev}} = \sum_{i=1}^{N_I} \left|U_{t,i}^2 - 1\right| \;\; (U_{t,i} \geq U_{\text{Max}} || U_{t,i} \leq U_{\text{Min}}) \qquad (14)$$

where $U_{t,i}$ is the voltage of node i at time t, and U_{Max} and U_{Min} are the voltage constraints. Subsequently, the SOP would mitigate the fault voltage after reconfiguration.

In details, during a system fault, the SOP can first provide independent fault voltage control via controlling the voltage waveform dynamically within milliseconds and then enabling transient control. Moreover, even without the help of active sources at the receiving end, the VSC can build its own voltage [14], [15]. If the system fault should be isolated, various control strategies can be applied to limit transient overvoltage and overcurrent of VSCs, by which that network disturbances or faults on one connected feeder can be isolated from the other side by VSCs [14], [16].

Networked MGs can promote self-healing capability of electricity systems. For abnormal system conditions, MGs can be used as extra generation capacity [17], [18]. Moreover, when a fault occurs inside the MG, it can be isolated but it can fully supply itself by switch operation modes and avoid bringing disruptions to the main grid [7], [18]. Thus, regarding the network reconfiguration scheme proposed in this article, the networked MGs can help reduce overall load curtailment by 1) be placed to vulnerable loads to offer extra generation and 2) providing supply restoration for isolated sub-systems.

F. PSO-Optimization-Based System Reconfiguration

In order to maintain proper switch operations for postcatastrophe electricity systems, a searching algorithm should be developed regarding all possible combinations. However, using normal 0-1 optimization may lead to combination explosion, even if the graph-theory-based circuit simplification method was applied, and there would still be an unduly amount of computation results. Hence, PSO optimization is applied to mitigate the complexity of the computation process.

The solution searching algorithm based on PSO can be classified as [19]–[22]

$$\begin{cases} P\text{best}_i = \min\left\{\sum_{k=1}^{n} LL_{\text{line}} + \sum_{k=1}^{m} LL_{\text{Buck}} + LL_{\text{iso}}\right\} \\ V_i^{t+1} = \alpha V_i^t + \beta_1 r_1 \left(P\text{best}_i - x_i^t\right) + \beta_2 r_2 \left(G\text{best}_i - x_i^t\right) \\ x_i^{t+1} = x_i^t + V_i^{t+1} \\ \alpha^{t+1} = \alpha_{\max} - t \times \frac{\alpha_{\max} - \alpha_{\min}}{t_{\max}} \\ S\left(V_i\right) = \frac{1}{1+e^{-V_i}} \\ V_{c,\text{Min}} \leq V_c \leq V_{c,\text{Max}} \\ I_{c,\text{Min}} \leq I_c \leq I_{c,\text{Max}} \\ r_1, r_2 = r \text{ and } \{0,1\} \\ \text{if } \; r_1, r_2 < S\left(V_i\left(t+1\right)\right), \; x_i^{t+1} = 1 \\ \text{if } \; \mathrm{r}_1, \mathrm{r}_2 > \mathrm{S}\left(\mathrm{V}_\mathrm{i}\left(\mathrm{t}+1\right)\right), \; x_i^{t+1} = 0 \end{cases} \qquad (15)$$

where $P\text{best}_i$ is the best position experienced by ith particle, $G\text{best}_i$ is the best particle of the entire population, V_i^t is the present velocity, x_i^t is the current position, α and β_1, and β_2 refer to inertia weight and weighting factors of the stochastic acceleration terms, respectively, r_1 and r_2 are numbers randomly chosen from a uniform distribution [0,1], V_c is the voltage constraint, I_c is the current constraint, and $S(V_i)$ is a sigmoid limiting transformation that can update particles velocity.

Regarding the post-disaster system, the combination of switch operations can be seen as the position experienced by particles. For instance, if there are 30 branches and 5 of them should be switched OFF, then each combination represents for a possible position and would be recorded by searching particles. In this article, the best position of PSO optimization is set to minimum load curtailment, and, subsequently, the reconfiguration scheme with minimum load curtailment would be proposed.

G. Weight of Load by PageRank

To classify the critical load that should be placed with MGs, the importance of each load should be distinguished. Hence, a load importance assessment method developed on the basis of the PageRank algorithm is applied.

The PageRank algorithm is a commonly used algorithm that quantifies the weight of pages in a web network. Since the weight of each node is related to both initial quality and linked nodes, the developed PageRank algorithm divides the weight proportional to each nodes' importance (its number of inlinks and outlinks). The importance of the number of inlinks and outlinks is defined as $w_{(v,u)}^{\text{in}}$ and $w_{(v,u)}^{\text{out}}$, respectively [23]

$$w_{(v,u)}^{\text{in}} = \frac{I_u}{\sum_{p\in R(v)} I_p} \tag{16}$$

$$w_{(v,u)}^{\text{out}} = \frac{O_u}{\sum_{p\in R(v)} O_p} \tag{17}$$

where I_u and I_p represent the number of inlinks of page u and page p, respectively. O_u and O_p are the number of outlinks of page u and page p. Additionally, page p is the reference page.

However, different from Web links that maintain the same weight among the entire network, branches of the energy system can carry a different amount of energy. Thus, for energy systems, I_u and I_p can be replaced with e_x^{out} and e_x^{in}, where e_x^{in} represents for the sum of inflow energy of node *x*, and e_x^{out} refers to the sum of outflow energy of node *x*.

Subsequently, the weight of system nodes can be written as

$$PR\left(u\right) = \left(1-a\right) + a \sum_{D_{(\text{in})u}} PR\left(v\right) eW_{(v,u)}^{\text{in}} eW_{(v,u)}^{\text{out}}. \tag{18}$$

III. DEMONSTRATION

A typical 33-bus electricity system with 3 SOPs and 2 networked MGs will be used to validate the proposed scheme. A dynamic hurricane model will be developed based on the work presented in [2] and [12], and both severity and probability are considered. The system reconfiguration scheme would be applied after the hurricane leaves this region.

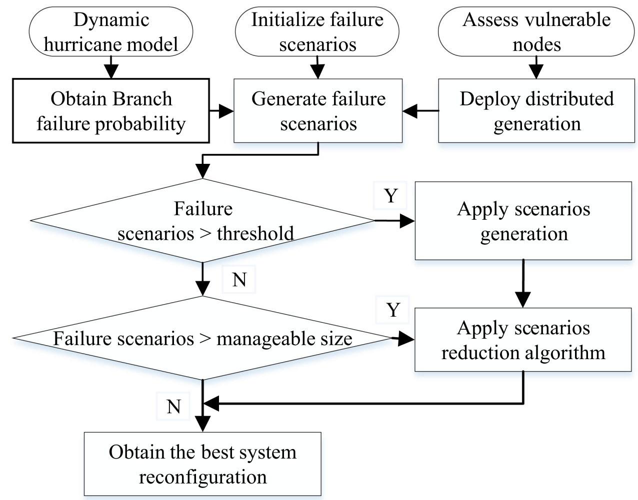

Fig. 3. Implementation of the proposed scheme.

TABLE I
IMPLEMENTATION STEPS

Implementation steps
1. Apply the PageRank algorithm to assess vulnerable nodes and deploy distributed generators.
2. Simulate failure rate for each branch.
3. If the number of failure scenarios is larger than the manageable size, apply scenarios reduction algorithm. And if the number of failure scenarios is less than the selected threshold, apply scenarios generation algorithm.
4. Choose the most possible failure scenarios as the assumed failure scenario.
5. Obtain load curtailment of the overall network.
6. Find the best reconfiguration strategy

Based on the simulation of the proposed hurricane model, the following step is to quantify the wind intensity that each branch would experience at each recorded time. Subsequently, possible failure scenarios of overall system branch loss are built according to (8)–(11). If the number of failure scenarios is bigger than 1000, only reduction algorithm will be used. If the number of possible scenarios is between 100 and 1000, scenario generation algorithm will be first used, followed by the scenario reduction algorithm. After 10 000 times of Monte Carlo simulation, 3 typical scenarios are selected to demonstrate the results. Finally, the PSO optimization is applied to find the most proper reconfiguration to mitigate load loss. The flowchart of implementation steps is shown as Fig. 3 and Table I.

IV. RESULT ANALYSIS

This section uses the following test system in Fig. 4 to demonstrate the designed model. The test system contains 33-bus, 3 networked MGs, and 5 SOPs, and the dashed line represents SOPs. The initial switch operation would be 32 switches normally opened and 5 switches normally closed.

This article has been accepted for inclusion in a future issue of this journal. Content is final as presented, with the exception of pagination.

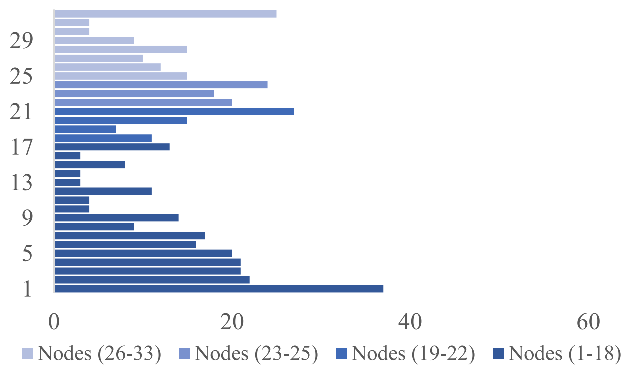

Fig. 4. The assessed importance of system nodes.

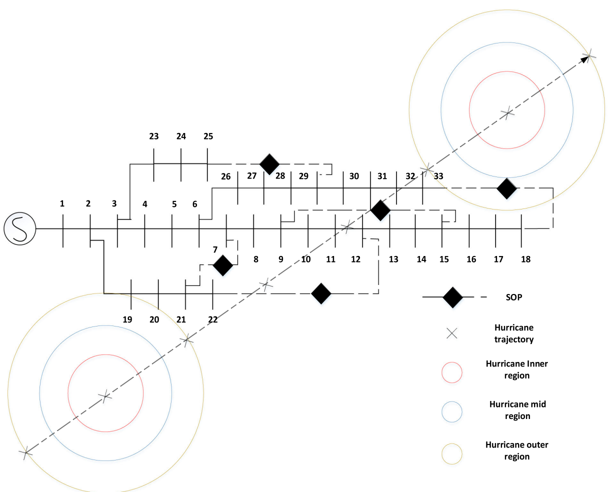

Fig. 5. The test system and simulated hurricane.

Fig. 4 shows the assessed importance of system nodes. It can be seen that except the balance node bus 1, the most vulnerable nodes are 22, 25, and 33. Additionally, this result shows the rank value of the test system when all the SOPs are switched ON. Thus, after assessing the importance of each node (with SOP installed), bus 22, bus 25, and bus 33 are selected to be replaced by networked MGs.

Consequently, since the networked MGs are capable to fully empower itself, even if buses 22, 25, and 9 are isolated from the main grid (by hurricane attack or reconfiguration), their load is completely curtailed. It is assumed that the hurricane path is linear across the whole grid. As shown in Fig. 5, the region inside the red circle is under the influence of maximum wind speed, whereas the region inside the blue circle and yellow circle maintains 82.5% and 50% impact of the maximum wind speed. The radius of the circles is 1, 2, and 3 km, respectively. For the modeled hurricane, the closer the system equipment to the center, the higher the hurricane intensity they would experience. Consequently, each electrical equipment would experience dynamic variational hurricane stress.

Fig. 5 shows areas affected by wind speed variation of the hurricane. As shown in Fig. 1, it can be seen that the hurricane intensity rises nearly 50% over time. Moreover, according to (8), each possible failure would result in more vulnerable system components at the next time stage. Thus, the upper east part of system branches may obtain a higher failure probability.

TABLE II
TIME-SERIES AFFECTED BRANCH

Time period (h)	Affected branch
3	N/A
6	N/A
9	2-19, 19-20, 20-21, 21-22, 7-21
12	5-6, 6-7, 6-26, 7-8, 8-9, 9-10, 10-11,11-12, 20-21, 21-22, 26-27, 27-28, 28-29
15	6-7, 7-8, 8-9, 9-10, 10-11, 11-12, 12-13, 13-14, 14-15, 18-33, 26-27, 27-28, 28-29, 29-30, 30-31, 31-32, 32-33
18	11-12, 12-13, 13-14, 14-15, 15-16, 16-17, 17-18, 18-33, 29-30, 30-31, 31-32, 32-33
21	18-33
24	N/A

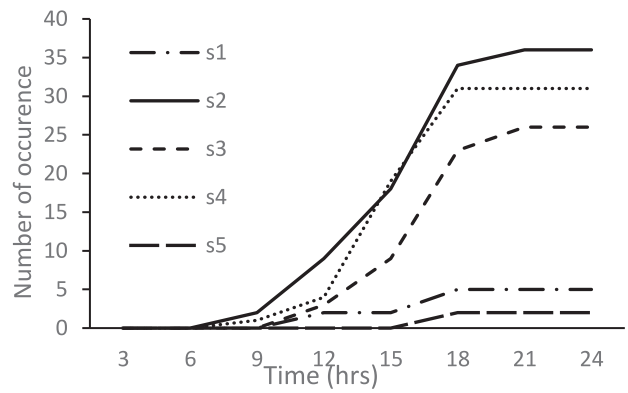

Fig. 6. The failure scenarios over 24 h.

The affected branches of each time period are listed in Table II. Since SOPs are operated under normal condition during hurricane attack, only 34 other branches would be affected, and, subsequently, the total failure scenarios would be 2^{34}.

The selected threshold $\sigma_{\rm thr}$ and manageable size $\sigma_{\rm man}$ are set to 1000 and 100, respectively. Subsequently, if failure scenarios were more than 1000, only reduction algorithm would be used, and if possible scenarios were between 100 and 1000, the scenario generation algorithm would be used first and then deploy the scenario reduction algorithm. After 10 000 times Monte Carlo simulation, 100 scenarios are classified as the most possible failure scenarios to be studied.

Since this is still an unduly amount of finding the best reconfiguration choice for these conditions, only three representative scenarios are selected to be used for validating the proposed strategy. The first scenario refers to minor damage, in which branches 6–7 and 32–33 are faulted transmission lines caused by hurricane attacks. The second and third scenarios correlate to more severe conditions, where the faulted lines are 9–10, 10–11, 28–29, 30–31, and 7–8, 17–18, 28–29, respectively. Fig. 6 shows the variation of possible failure scenarios over 24 h, where s1–s5 represent the scenarios of 1 failure branches to 5 failure branches, respectively. Furthermore, owing to the rising wind speed, possible failure scenarios would increase rapidly between 12 and 18.

TABLE III
RECONFIGURATION RESULT FOR SCENARIO ONE

	Before Reconfiguration	After Reconfiguration
Switched off branches	6-7, 32-33	6-7, 9-15, 11-12, 25-29, 32-33
In used SOPs	N/A	8-21, 12-22, 18-33
MG supply (MW)	0	1.3
Load curtailment (MW)	3.03	1.49
Curtailment reduction	N/A	50.69%

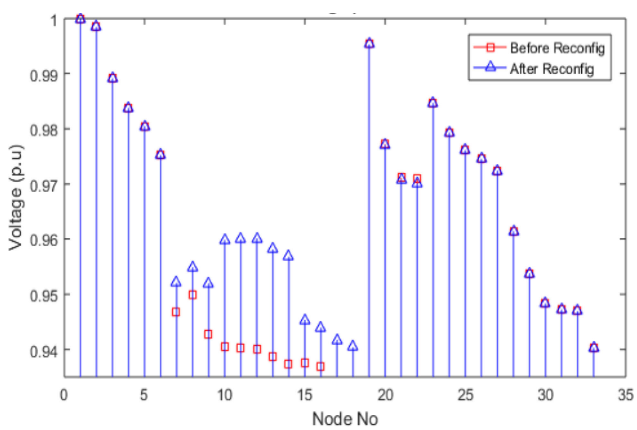

Fig. 7. The voltage magnitude for system nodes.

A. First Scenario

In this scenario, branch 6–7 and branch 32–33 are destroyed by hurricane attack, which means branches 6–7 and 32–33 cannot be reswitched ON at any time. Thus, including five SOPs, there are three switched-OFF branches before reconfiguration starts.

Consequently, according to the assumption before, only five branches of the test system are allowed to be switched OFF, and the purpose of system reconfiguration under two damage branch condition would be searching for possible switch operation that relates to lowest load curtailment. With the help of the PSO optimization, the best solution is switching OFF branches 9–15, 11–12, and 25–29. Consequently, the supply restoration mode SOPs would be 8–21, 12–22, and 18–33. Since no load get isolated from the main grid, the networked MGs are still fixed to provide an extra capability for system vulnerable nodes. The overall generation of networked MGs is 1.3 MW, the sum of the maximum capacity of all MGs. Subsequently, all the MGs are fully allocated to restore curtailed load demand. Thus, to summarize, based on SOPs and Networked MGs, the reconfiguration scheme recovers 50. 69% of the curtailed load.

As shown in Table III, by changing the system topological structure, the load curtailment owing to hurricane disturbance is mitigated from 3.03 to 1.49 MW. The efficiency of this reconfiguration is relatively high and may relate to the system that maintains a radial structure with no isolated load.

Fig. 7 shows voltage at all nodes. Most of the loads obtain their previous voltage value, whereas branches between node 8 and node 11 and branches between node 12 and node 18 obtain increasing voltage. Relating to the change of branch connection, the increasing voltage is caused by the separation of branch 7–18. Consequently, other branches that maintain the same voltage as before can be related to the voltage deviation offered by SOPs.

TABLE IV
FIRST RECONFIGURATION RESULT FOR SCENARIO TWO

	Before Reconfiguration	After Reconfiguration
Switched off branches	9-10, 13-14, 28-29, 30-31	N/A
Load curtailment (MW)	Total	N/A
Load curtailment reduction	N/A	N/A

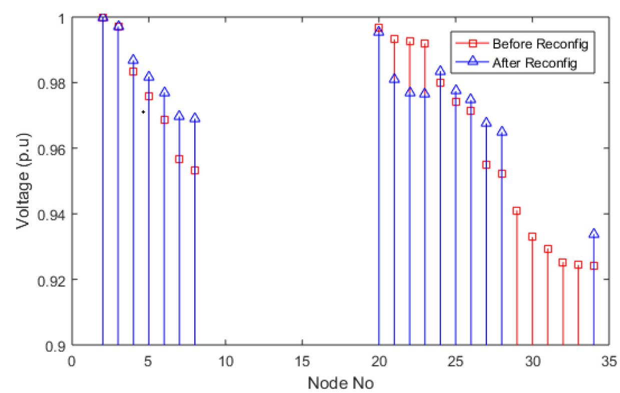

Fig. 8. The voltage magnitude for system nodes.

TABLE V
SECOND RECONFIGURATION RESULT FOR SCENARIO TWO

	Before Reconfiguration	After Reconfiguration
Switched off branches	9-10, 13-14, 28-29, 30-31	9-10, 13-14, 28-29, 30-31, 9-15, 8-21
In used SOPs	N/A	25-29, 12-22, 18-33
Overall MG supply (MW)	0	0.78
Load curtailment (MW)	Total	1.23
Load curtailment reduction	N/A	30.75%

B. Second Scenario

For the second scenario, as Table IV illustrated the reconfigure algorithm failed, and even if the branches are arranged to higher capacity with more flexible constraints, the algorithm can still not offer a solution. Thus, it seems not possible to reconfigure the test system with the limit of only five switches can be operated.

If ignoring the constraint of allowed switch operation, a possible solution would be, as Fig. 8 and Table V illustrated, reconfigure the system with branches 9–15 and 8–21 switched OFF and

TABLE VI
RECONFIGURATION RESULT FOR SCENARIO THREE

	Before Reconfiguration	After Reconfiguration
Switched off branches	7-8, 17-18, 28-29	7-8, 8-21, 12-22, 17-18, 28-29
In used SOPs	N/A	9-15, 18-33, 25-29
Overall MG supply (MW)	0	0.87
Load curtailment (MW)	3.86	2.51
Load curtailment reduction	N/A	34.97%

then schedule networked MGs to restore isolated subsystems. According to this plan, the in-used SOPs are 25–29, 12–22, and 18–33. Although buses 14–18 and 31–33 are isolated into two island systems, the SOPs 18–33 connect them together and allow them to be supplied by rescheduled MGs. Subsequently, the MGs placed in buses 22 and 25 (the other MG has already be deployed to bus 33) are rerouted to restore the islanded subsystem, and the overall reconfigure efficiency would be 30.75%.

C. Third Scenario

Although only three branches are disturbed by hurricane activities, the load curtailment owing to hurricane disturbance is 3.86 MW, nearly the total load of this system. Caused by hurricane attack, this condition may relate to two islanded subsystems, buses 29–33 and buses 8–17. It can also be seen in Table VI that only buses 29-33 are restored from island mode by reconfiguration, which may refer to the limited capacity of SOPs 7–21 and 12–22, which cannot fully supply the load demand of buses 8–17.

Then, since buses 8–17 are islanded, the system must enter the MG coordination mode that all networked MGs should be allocated to restore the islanded subsystem. Assuming the branches that connect network MGs and isolated circuits would not be overloaded, the curtailed load demand would be completely restored (0.87MW) owing to MG coordination.

Since all the networked MGs are coordinated to restore the isolated buses 8–17, the supply to the main grid decreases, and the reconfigure efficiency, 34.97%, is relatively low. Thus, the final load restoration for this scenario would be 1.35 MW, which not only includes loss load recovery based on system reconfiguration but also refers to restored islanded subsystems by MG allocation.

Fig. 8 shows the voltage profile of system nodes before and after reconfiguration. Since the hurricane attack leads to the isolation of buses 8–17 and buses 29–33, the voltage profiles before reconfiguration of these nodes are not recorded, whereas for the reconfigured system, the voltage profiles of islanded buses, buses 8–17, are ignored.

Fig. 9 shows the cumulative distribution function (CDF) of load curtailment for 100 scenarios, and it can be seen that the most rapid growth of this cumulative probability appears between 3.6 and 4 MW. And the confidence interval is between

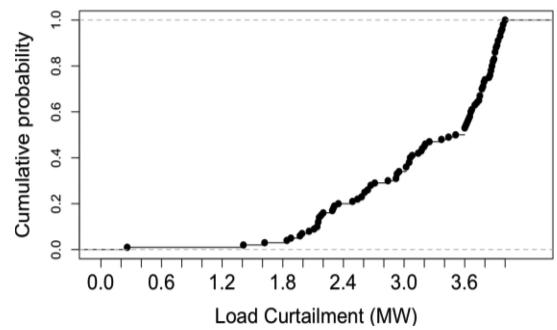

Fig. 9. The cumulative probability of overall load curtailment.

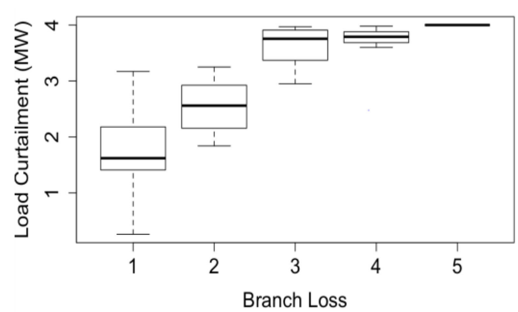

Fig. 10. The load curtailment per branch loss.

2.2 and 4.0 MW, which indicates that the most possible load loss caused by this modeled hurricane would be 2.2–4.0 MW. Fig. 10 illustrates load curtailment against the number of branch loss. The black bar in each box is its median value of load curtailment, and the box describes its upper and lower boundaries. According to the simulated results, if two branches are damaged by the hurricane, the median value of load curtailment is around 1.5 MW, and the minimum and maximum are approximately 1.4 MW and 2.2 MM, respectively. For the cases with four branches lost, the median value and upper, lower, quartile values are very close, and thus it can be concluded that the load curtailment due to four branches loss is close to 3.75 MW. The consequence becomes worse for the cases with five branches lost, with median, minimum, and maximum almost overlap at the value of 4 MW.

It is noted that all electricity branches are assumed to be installed with switches, and this is the case in practice. In order to fast and reliably reconfigure distribution systems, many SOPs have been installed because of their best performance. Thus, it is feasible to implement our proposed method in practice. In terms of reliability, as it acquires data from supervisory control and data acquisition (SCADA) and, thus, should be cyber secured. However, in some cases, the algorithm of PSO might take longer time to find optimal solutions and, in the worst case, might not converge due to the high dimensionality and complexity of the problem. These issues can compromise the reliability of the system. However, there are backup optimization methods that can be designed to complement the proposed approach to ensure the robustness of the system, and this is the research problem we will explore.

V. CONCLUSION

This article proposes a two-stage scheme to enhance distribution system resilience against hurricanes with coupling SOPs and networked MGs.

Through extensive demonstration, the key findings are the following.

1) A variational hurricane event with regional time-series wind intensity can cause certain load curtailment, and the consequences are decided by the importance of load.
2) The reconfiguration of postdisaster power systems facilitated by the installation of SOPs and networked MGs can help minimize load curtailment.
3) Based on the coordination of SOPs and networked MGs, temporary restoration can be applied to mitigate the loss until possible repairs can be taken, and thus system resilience can be enhanced

This work provides system operators with a powerful tool to enhance the resilience of distribution systems under extreme hurricane events with reduced load loss. Thus, least costly investment is needed in the system, which would eventually benefit customers with enhanced security but low bills.

REFERENCES

[1] Y. Lin, B. Chen, J. Wang, and Z. Bie, "A combined repair crew dispatch problem for resilient electric and natural gas system considering reconfiguration and DG islanding," *IEEE Trans. Power Syst.*, vol. 34, no. 4, pp. 2755–2767, Jul. 2019.

[2] S. Ma, B. Chen, and Z. Wang, "Resilience enhancement strategy for distribution systems under extreme weather events," *IEEE Trans. Smart Grid*, vol. 9, no. 2, pp. 1442–1451, Mar. 2018.

[3] A. M. Salman, Y. Li, and M. G. Stewart, "Evaluating system reliability and targeted hardening strategies of power distribution systems subjected to hurricanes," *Rel. Eng. Syst. Saf.*, vol. 144, pp. 319–333, 2015.

[4] D. N. Trakas, M. Panteli, N. D. Hatziargyriou, and P. Mancarella, "Spatial risk analysis of power systems resilience during extreme events," *Risk Anal.*, vol. 39, pp. 195–211, 2019.

[5] K. P. Schneider, F. K. Tuffner, M. A. Elizondo, C.-C. Liu, Y. Xu, and D. Ton, "Evaluating the feasibility to use microgrids as a resiliency resource," *IEEE Trans. Smart Grid*, vol. 8, no. 2, pp. 687–696, Mar. 2017.

[6] Z. Wang and J. Wang, "Self-healing resilient distribution systems based on sectionalization into microgrids," *IEEE Trans. Power Syst.*, vol. 30, no. 6, pp. 3139–3149, Nov. 2015.

[7] Y. Tan, F. Qiu, A. K. Das, D. S. Kirschen, P. Arabshahi, and J. Wang, "Scheduling post-disaster repairs in electricity distribution networks," *IEEE Trans. Power Syst.*, vol. 34, no. 4, pp. 2611–2621, Jul. 2019.

[8] W. Cao, J. Wu, N. Jenkins, C. Wang, and T. Green, "Operating principle of soft open points for electrical distribution network operation," *Appl. Energy*, vol. 164, pp. 245–257, 2016.

[9] P. L. M. De Vet, R. T. Mccall, J. P. Den Bieman, M. J. Stive, and M. Van Ormondt, "Modelling dune erosion, overwash and breaching at Fire Island (NY) during hurricane sandy," in *The Proc. of the Coas. Sedi. 2015*, Singapore: World Sci., 2015.

[10] M. Ouyang and L. Duenas-Osorio, "Multi-dimensional hurricane resilience assessment of electric power systems," *Struct. Saf.*, vol. 48, pp. 15–24, 2014.

[11] J. Winkler, L. Duenas-Osorio, R. Stein, and D. Subramanian, "Performance assessment of topologically diverse power systems subjected to hurricane events," *Rel. Eng. Syst. Saf.*, vol. 95, pp. 323–336, 2010.

[12] S. Ma, B. Chen, and Z. Wang, "Resilience enhancement strategy for distribution systems under extreme weather events," *IEEE Trans. Smart Grid*, vol. 9, no. 2, pp. 1442–1451, Mar. 2018.

[13] M. W. Horner and J. A. Downs, "Optimizing hurricane disaster relief goods distribution: Model development and application with respect to planning strategies," *Disasters*, vol. 34, pp. 821–844, 2010.

[14] W. Cao, J. Wu, N. Jenkins, C. Wang, and T. Green, "Benefits analysis of soft open points for electrical distribution network operation," *Appl. Energy*, vol. 165, pp. 36–47, 2016.

[15] C. Trujillo, D. Velasco, J. Guarnizo, and N. Díaz, "Design and implementation of a VSC for interconnection with power grids, using the method of identification the system through state space for the calculation of controllers," *Appl. Energy*, vol. 88, pp. 3169–3175, 2011.

[16] B. Jacobson *et al.*, "HVDC with voltage source converters and extruded cables for up to ±300 kV and 1000 MW," CIGRÉ Session, Montreal, QC, Canada, 2006, Paper B4-105.

[17] B. Chen, C. Chen, J. Wang, and K. L. Butler-Purry, "Sequential service restoration for unbalanced distribution systems and microgrids," *IEEE Trans. Power Syst.*, vol. 33, no. 2, pp. 1507–1520, Mar. 2018.

[18] Z. Wang, B. Chen, J. Wang, and C. Chen, "Networked microgrids for self-healing power systems," *IEEE Trans. Smart grid*, vol. 7, no. 1, pp. 310–319, Jan. 2016.

[19] Z.-K. Li, X.-Y. Chen, K. Yu, H.-M. Liu, and B. Zhao, "Hybrid particle swarm optimization for distribution network reconfiguration," vol. 28, pp. 35–41, *Proc. CSEE*, 2008.

[20] T. Niknam, "An efficient hybrid evolutionary algorithm based on PSO and HBMO algorithms for multi-objective distribution feeder reconfiguration," *Energy Convers. Manage.*, vol. 50, pp. 2074–2082, 2009.

[21] D. Das, "A fuzzy multiobjective approach for network reconfiguration of distribution systems," *IEEE Trans. Power Del.*, vol. 21, no. 1, pp. 202–209, Jan. 2006.

[22] A. M. Imran and M. Kowsalya, "A new power system reconfiguration scheme for power loss minimization and voltage profile enhancement using fireworks algorithm," *Int. J. Elect. Power Energy Syst.*, vol. 62, pp. 312–322, 2014.

[23] Y. Shen, C. Gu, and P. Zhao, "Structural vulnerability assessment of multi-energy system using a PageRank algorithm," *Energy Procedia*, vol. 158, pp. 6466–6471, 2019.

Yichen Shen (Student Member, IEEE) was born in Hebei, China. He received the double bachelor's degree in electrical engineering in 2017 from North China Electric Power University, China, and the University of Bath, U.K., where he is currently working toward the Ph.D. degree in the University of Bath.

His research interest includes resilient multienergy systems.

Chenghong Gu (Member, IEEE) was born in Anhui, China. He received the master's degree in electrical engineering from Shanghai Jiao Tong University, Shanghai, China, in 2007, and the Ph.D. degree from the University of Bath, Bath, U.K.

He is currently a Lecturer and an EPSRC Fellow with the Department of Electronic and Electrical Engineering, University of Bath. His major research interests include multivector energy system, smart grid, and power economics.

Zhibo Ma received the B.Sc. degree from Sichuan University, Chengdu, China, in 2007, and the M.Sc. degree in power systems, and the Ph.D. degree from the University of Bath, Bath, U.K., in 2008 and 2016, respectively.

Since 2009, he has worked on various positions with National Grid, London, U.K., where he is currently a Senior Power System Engineer with Electricity Control Center. His current research interests include smart grids, renewable energy, and system control.

Xinhe Yang (Student Member, IEEE) was born in Fujian, China. He received the B.Eng. degree in electrical engineering from the University of Bath, Bath, U.K., and the B.Eng. degree in electrical power engineering from North China Electric Power University, Beijing, China, both in 2016. He is currently working toward the Ph.D. degree in the University of Bath.

His main research interests include power system planning and power system economics.

Pengfei Zhao (Student Member, IEEE) was born in Beijing, China. He received the double B.Eng. degree from the University of Bath, U.K., and North China Electric Power University, China, in 2017. He is currently working toward the Ph.D. degree in the University of Bath, Bath, U.K.

He was a Visiting Ph.D. Student with Smart Grid Operations and Optimization Laboratory, Tsinghua University, Beijing, China, in 2019. His research interests include the operation and planning of integrated energy systems.